Structural Phase Transition and Compressibility of CaF_2 nanocrystals under High Pressure

Jingshu Wang[1], Jinghan Yang[1], Tingjing Hu[1], Jihui Lang[1]*, Xiaoxin Wu[1], Junkai Zhang[1], Haiying Zhao[1], Jinghai Yang[1] and Qiliang Cui[2]

[1] Key Laboratory of Functional Materials Physics and Chemistry of the Ministry of Education, National Demonstration Center for Experimental Physics Education, Jilin Normal University, Siping 136000, Jilin, China.

[2] State Key Laboratory of Superhard Materials, Jilin University, Changchun 130012, China.

* Correspondence: 47612697@qq.com

Supporting Information

1. Synthesis details of 8 and 23 nm CaF_2 nanocrystals

The 8 nm CaF_2 nanocrystals were prepared by a liquid-solid-solution (LSS) phase transfer synthetic strategy. Oleic acid, ethanol, and sodium hydroxide were mixed together, the reactants of 0.1 mol/L $Ca(NO_3)_2$ and 0.15 mol/L NaF were added to the mixture under vigorous stirring for 1 h and then transferred into a 40 ml autoclave, sealed and hydrothermally treated at temperature of 160 °C for 24 h.

For the 23 nm CaF_2 nanocrystals, we adopted a typical hydrothermal synthesis method choosing ethanol as solvent. 0.5 mmol of $Ca(NO_3)_2$ and 1 mmol of NaF were dissolved in 10 ml distilled water to form clear solutions, respectively. The two solutions were mixed under full stirring to obtain opaque white suspension. The solution was transferred in to a 40ml autoclave which was filled to 85% of its total capacity with ethanol. Then, the system kept in an oven at 140 °C for 15 h.

The 8 nm and 23 nm CaF_2 nanocrystals were prepared by different synthetic methods.

2. For the 8 nm-sized CaF_2 nanocrystals, with B_0' fixed at 4, we can yield the bulk modulus B_0 of 112(6) GPa for the fluorite structure and B_0 of 93(9) GPa for the α-$PbCl_2$-type structure (Fig.1s). The isothermal bulk modulus of the fluorite phase and α-$PbCl_2$-type phase are both significantly larger than those of the bulk CaF_2 and 23 nm-sized CaF_2 nanocrystals (this work), indicating the highly incompressibility of smaller size CaF_2 nanocrystals.

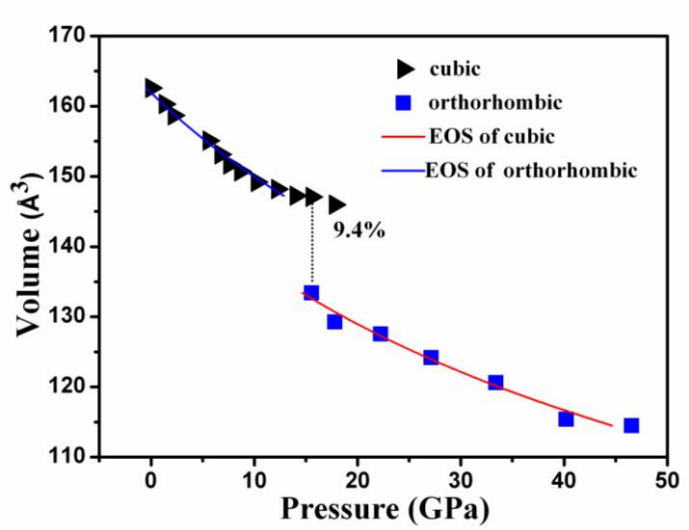

Fig.1s. The volumes per formula unit of the various phases of 8 nm-sized CaF_2 nanocrystals as a function of pressure at room temperature.

3. For further analysis, we have carried out HRTEM analysis of 8 nm CaF_2 nanocrystals (Fig. 2s). The HRTEM result showed that the sample has no visible defects and dislocations, indicating relatively low defects concentration. The elevation of the phase transition pressure in 8 nm-sized CaF_2 nanocrystals is considered to be mainly due to the grain size effect. In this work, the HRTEM image of the 23 nm CaF_2 nanocrystals showed that sample contains visible structural impurities like dislocations and defects. These dislocations and defects could act as the weak points and induce stress concentration, so a new high-pressure phase prefers to nucleate at such defect sites. Therefore, high pressure phase nucleated in a defected crystal certainly has a reduced nucleation pressure relative to that in an ideal defect free crystal.

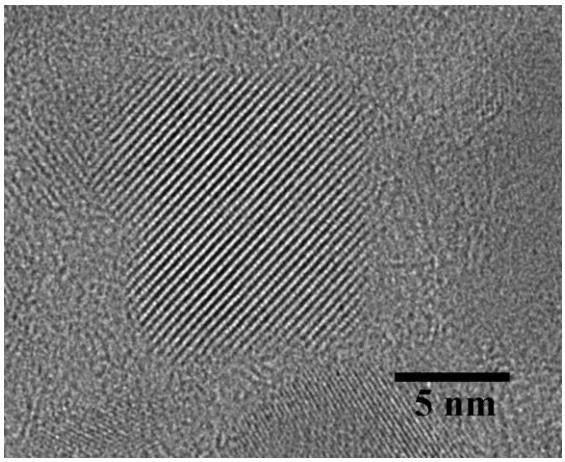

Fig.2s. HRTEM image of the as-synthesized 8 nm CaF_2 nanocrystals.

4. Table 1s exhibits the phase transition, unit cell volume at ambient pressure and volume collapse of CaF_2 materials, which clearly revealed the differences between bulk and nanoscale CaF_2.

As shown in Table Is, the volume collapse of the 23 nm CaF_2 nanocrystals is

closer to that in bulk and 8 nm CaF_2. That is, a large volume collapse in 23 nm CaF_2 does not lead to a reduction of P_T. The volume of 23 nm CaF_2 has obvious expansion at ambient, which most likely caused by the defects and dislocations, and this deduction is consistent with TEM characterization. Based on the above discussions, the defects and dislocations may be the most important factor to affect the structural stability in 23 nm CaF_2.

TABLE 1s. Transition Pressure (P_T), unit cell volume (V_0) and volume collapse $\triangle V$(%).

morphology	size	P_T (GPa)	V_0(Å^3)	$\triangle V$(%)
bulk	Micro	8-10	163.0(4)	8-11
nanocrystals	8 nm	14	162.7(7)	9.4%
This work	23 nm	9.5	166.7(2)	9.6%